



ELSEVIER

Physica B 291 (2000) 89–96

PHYSICA B

www.elsevier.com/locate/physb

# Magneto-optic activity of f–d and f–f electron transitions in Pr<sup>3+</sup> in the glass matrix LiB<sub>3</sub>O<sub>5</sub>

A.M. Potseluyko\*, I.S. Edelman, V.N. Zabluda, O.A. Bolsunovskaya, A.V. Zamkov, S.A. Parshikov, A.I. Zaytsev

*L.V. Kirensky Institute of Physics, SB RAS, 660036 Krasnoyarsk, Russia*

Received 23 June 1999; received in revised form 12 August 1999; accepted 11 November 1999

## Abstract

The results of absorption, Faraday rotation and magnetic circular dichroism measurements for glasses with the composition of LiB<sub>3</sub>O<sub>5</sub> + Pr<sub>2</sub>O<sub>3</sub> are presented. The effective wavelength of the transition giving the main contribution to Faraday rotation in these glasses is determined. The contributions of several f–f transitions to Faraday rotation are separated and their magneto-optical activities are evaluated in comparison with the activity of the f–d transition. © 2000 Elsevier Science B.V. All rights reserved.

*Keywords:* Faraday rotation; Magneto-optic activity; Praseodymium

The f<sup>n</sup> electron configuration of lanthanide ions has been studied in detail, both experimentally and theoretically (see, for example, Ref. [1]). But the investigation of the intensities of intraconfigurational f–f transitions of trivalent lanthanide ions in different matrices is of importance up to now because the spectral intensities can help in understanding the interaction between the lanthanide and the surrounding ions. The additional information about the interaction can be obtained with the help of Faraday effect, which includes Faraday rotation (FR) and magnetic circular dichroism (MCD). The FR is a rotation of the polarization plane of the linearly polarized electromagnetic wave propagating in a medium parallel to the

direction of an applied magnetic field. MCD is a difference of the optical densities of the medium for the left and right circularly polarized waves propagating along the magnetic field direction. The FR and MCD are related over a given frequency interval by the Kramers–Kronig transforms. Due to their spectral dependencies MCD is studied preferentially from the fundamental point of view, while the FR is used for practical applications in different magneto-optical devices. In the first case an investigator deals with f–f electron transitions and in the second case f–d transitions play the main role.

High concentrated rare-earth (RE) glasses are considered as an effective magneto-optical material [2–5]. From this point of view some Pr-containing glass compositions were shown to be one of the best magneto-optical materials for the ultra-violet (UV) spectral region [3]. There are several papers also devoted to the magneto-optical spectra of Pr

\*Corresponding author. Fax: +7-3912-438923.  
E-mail address: ise@iph.krasnoyarsk.su (A.M. Potseluyko).

containing glasses in the region of f–f transitions. The MCD and FR spectra were studied in praseodymium-doped soda glass [6], and in Refs. [7,8] in fluorozirconate glasses.

The paper presented is devoted to the comparative investigation of magneto-optical effects and spectral intensities of the f–d and f–f  $\text{Pr}^{3+}$  electron transitions in a lithium–borate glass matrix. This matrix is transparent in UV up to 160 nm [9], what allows us to hope to distinguish the f–d transition in the  $\text{Pr}^{3+}$  absorption spectrum.

Glasses were prepared from the mixture of reagents:  $\text{Li}_2\text{B}_4\text{O}_7$ ,  $\text{B}_2\text{O}_3$  and  $\text{Pr}_6\text{O}_{11}$ . About 40 g batches were placed into a carbon crucible and heated at  $1100 \pm 50^\circ\text{C}$  in the Ar gas. During this process  $\text{Pr}^{4+}$  from the compound with the mixed valency was reduced to  $\text{Pr}^{3+}$  so the final glass composition can be described by the formula  $\text{LiB}_3\text{O}_5 + x\text{Pr}_2\text{O}_3$ . The absence of  $\text{Pr}^{4+}$  ions in the glass synthesized is confirmed by the fact that only  $\text{Pr}^{3+}$  f–f-bands are observed in the glass absorption spectra as it will be seen further. The melt was vitrified by rapid cooling to  $350\text{--}400^\circ\text{C}$  and then the glasses obtained were annealed at  $300^\circ\text{C}$ . Measurements were made on polished glass samples of the thickness from 0.5 to 1.1 mm.

The Pr-ion molar concentration and the number of Pr-ions per  $\text{cm}^3$  are presented in Table 1. The concentration of Pr-ions per volume was calculated from the glass densities and composition.

The FR measurements were made by the null-analyzer method with the light wave polarization plane modulation [11] in the wavelength ranging from 230 to 1200 nm and at the value of the applied magnetic field changed from 2.65 to 5.0 kOe. The experimental error of the rotation angle measurement was within 0.2 min. On the basis of this

measurements the value of the Verdet constant  $V = \alpha/Hd$  was found, where  $H$  is the magnetic field in Oe,  $d$  is the sample thickness in cm and  $\alpha$  is the FR value in minutes, giving  $V$  the units of  $\text{min Oe}^{-1} \text{cm}^{-1}$ . Optical absorption measurements were made using a UVICON 943 spectrophotometer in the 180–900 nm wavelength region and on a Specord-20 in the region 900–1200 nm. Besides, MCD was measured in the region of the f–f transition for some samples using the modulation of light polarization with a piezooptic modulator [12]. All measurements were carried out at room temperature.

Fig. 1 shows the absorption spectra of a series of glasses containing Pr: (1) 0.73, (2) 5.13 and (3) 11.46 mol% (curves 2–4, correspondingly) and for the undoped glass matrix (curve 1). The wavelength of the fundamental band edge ( $\lambda_0$ ) of the samples 2 and 3 is  $\sim 250$  nm, which is a little longer in comparison with the corresponding wavelength in Refs. [3,5], and is considerably shorter in comparison with Ref. [2]. It is obvious, that the fundamental band edge is caused by Pr as the glass matrix is transparent through the whole spectral region investigated (curve 1). For the sample with the minimum Pr concentration we succeed to distinguish the band, which corresponds to the transition  $4f^2 \rightarrow 4f^1 5d^1$  with the center at 217 nm. Increasing the Pr concentration leads to involving other types of transitions in Pr-ions into the absorption process and against their background the f–d transition becomes indistinguishable. We assume, that the intensity of the f–d band is proportional to the Pr concentration, and use this assumption to evaluate its contribution to the absorption for the samples with 5.13 and 11.46 mol% Pr. These intensities are equal to  $\sim 1.91 \times 10^5$  and

Table 1  
Properties and parameters of the investigated glasses<sup>a</sup>

Number of sample	$c$ (mol %)	$N$ ( $10^{21}$ ion/ $\text{cm}^3$ )	$gJ(J+1)$	$\lambda_{\text{eff}}$ (nm)	$\lambda_0$ (nm)	$C_{\text{eff}}$ ( $10^{-38}$ erg $\text{cm}^3$ )	$\chi$ ( $10^{-5}$ )
1	5.13	1.37	16	217	249	20	1.22
2	11.46	3.27	16	217	256	20	2.91

<sup>a</sup>Note: ( $c$ ) molar concentration of Pr ions; ( $N$ ) number of Pr ion per volume;  $\lambda_{\text{eff}}$ -effective transition wavelength; ( $\lambda_0$ ) wavelength of absorption edge; ( $C_{\text{eff}}$ ) effective probability of electron transition;  $\chi = (Ng^2J(J+1)\mu_B^2/3kT)$  — magnetic susceptibility [10].

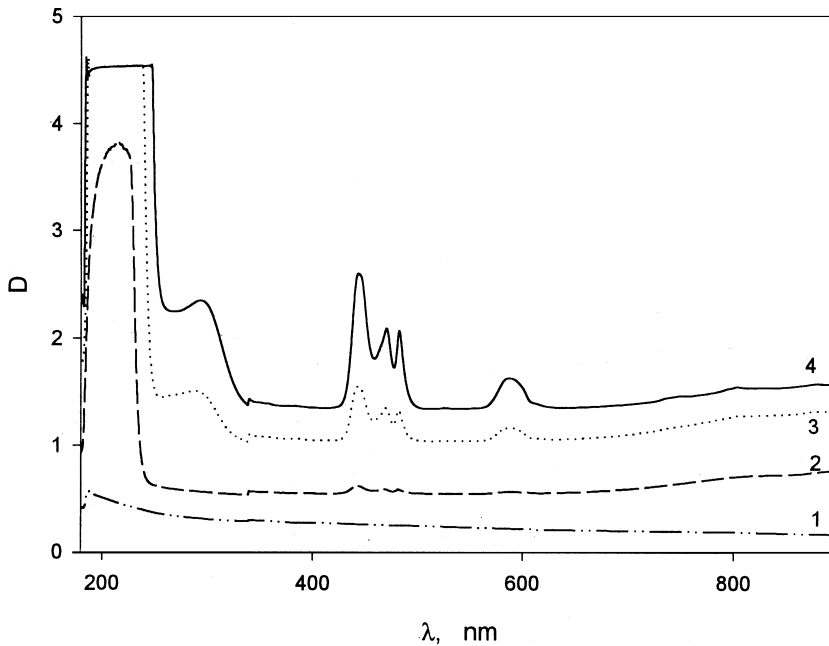


Fig. 1. Spectra of the optical density for the glass matrix (1) and the samples: (2) 0.73, (3) 5.13 and (4) 11.46 mol% Pr.  $D = \log(I_0/I)$ , where  $I_0$  and  $I$  are intensities of the incident and transmitted light.

$\sim 4.28 \times 10^5 \text{ cm}^{-2}$ , respectively. Unfortunately, the broad shoulder is observed near the fundamental band edge for the samples with a high Pr concentration which is not typical for  $\text{Pr}^{3+}$  bands (note the absence of the shoulder in the spectrum of the sample containing 0.73 mol% Pr). There are not enough data now to make a definite conclusion about the origin of this shoulder.

The character of the  $\text{Pr}^{3+}$  f-f absorption coincides in general with the results of other authors (for example, Ref. [5]). But, the f-f bands in the region from 400 to 500 nm, in our case, shift a little to longer wavelengths. Note that only three bands are observed in this region for the matrix investigated while in the case of single crystals usually four bands are resolved [13]:  ${}^3\text{P}_0$ ,  ${}^3\text{P}_1$ ,  ${}^1\text{I}_6$  and  ${}^3\text{P}_2$ .

Fig. 2 illustrates the Verdet constant dependence on the wavelength  $\lambda$  in the region from 375 to 650 nm for samples 1 and 2 and for the glass matrix (curve 3). The value of the Verdet constant, reduced to the Pr molar concentration, in the short wavelength region in the glasses considered is al-

most 1.8 times larger than the analogous value in Ref. [5]. In the insertion in this figure the Verdet constant dependence on wavelength is shown for the spectral region 200–340 nm for a sample containing 11.46 mol% Pr.

The dependence of the  $V(\lambda)$  obtained is typical for glasses, whose diamagnetic matrix is activated by paramagnetic RE ions, and it may be described theoretically by Van Vleck and Hebb [10]. Hence, the Verdet constant  $V$  can be expressed as

$$V = V_m + V_{re}, \quad (1)$$

where  $V_m$  is the Verdet constant of the diamagnetic matrix and  $V_{re}$  is the Verdet constant due to the paramagnetic RE ions. The latter can be expressed as

$$V_{re} = \left(\frac{A}{T}\right) NgJ(J+1) \sum_n \frac{C_n}{1 - \lambda^2/\lambda_n^2}, \quad (2)$$

where  $A = 1.53 \times 10^{16} \text{ (min grad Oe}^{-1} \text{ cm}^{-1} \text{ erg}^{-1})$  is a constant,  $T$  is the absolute temperature,  $N$  is

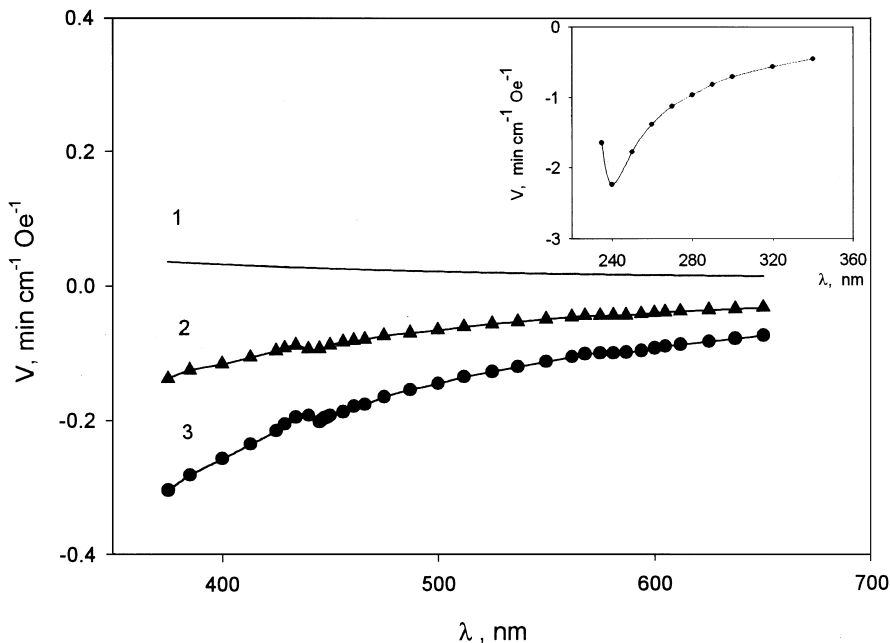


Fig. 2. Spectra of Verdet constant: (1) glass matrix, (2) 5.13, and (3) 11.46 mol% Pr. The inset shows Verdet constant for the samples with 11.46 mol% Pr.

the number of Pr ions in  $\text{cm}^3$ ,  $g$  is the Lande factor,  $J$  is the total angular momentum quantum number of the ground state,  $C_n$  is the relative transition probability,  $n$  is an index which runs over all the quantum numbers (except for the magnetic quantum number) of the excited states,  $\lambda$  is the light wavelength, and  $\lambda_n$  is the resonant wavelength. The summation over all the resonant wavelengths  $\lambda_n$  in Eq. (2) gives some effective wavelength  $\lambda_{\text{eff}}$ , corresponding to the transition, which gives the basic contribution to FR.

Then, we may write for the Verdet constant of paramagnetic RE ions

$$V_{\text{re}} = \left(\frac{A}{T}\right) N g J (J + 1) C_{\text{eff}} \left(1 - \frac{\lambda^2}{\lambda_{\text{eff}}^2}\right)^{-1}, \quad (3)$$

where  $C_{\text{eff}} = \sum_n C_n$ , or

$$V_{\text{re}} = B \left(1 - \frac{\lambda^2}{\lambda_{\text{eff}}^2}\right)^{-1}, \quad (4)$$

where  $B = (A/T) N g J (J + 1) C_{\text{eff}}$ .

Taking into account (1), the contribution of  $\text{Pr}^{3+}$  ions to the  $V$  value measured was obtained from the difference between the  $V$  value for the glass matrix and for the glass containing Pr. Then, the values  $V_{\text{re}}^{-1}$  were found and their dependencies on  $\lambda^2$  were plotted (Fig. 3). These dependencies, on the whole, are linear according to (4). In the region of f–f transitions the singularities of the S-shaped type are observed, which will be discussed later. The linear approximation of the curves gives us the value of the effective wavelength  $\lambda_{\text{eff}}$  (see Table 1 and Fig. 3). The value of  $\lambda_{\text{eff}}$  coincides for both samples 1 and 2 in Fig. 3 and is equal to 217 nm, which coincides also with the result of Ref. [5], but less, than  $\lambda_{\text{eff}}$  in Ref. [2]. Note, that the value  $\lambda_{\text{eff}}$  corresponds exactly to the wavelength of the f–d transition, which is observed in the absorption spectrum for the sample containing 0.73 mol% Pr (see Fig. 1, curve 2). Moreover, for a very thin sample we succeeded to obtain the FR curve in the region of the f–d transition with the characteristic bend near  $\lambda_{\text{eff}}$  (see Ins. in Fig. 2). If  $\lambda_{\text{eff}}$  is known we may obtain the coefficient  $B$  for the f–d transition in

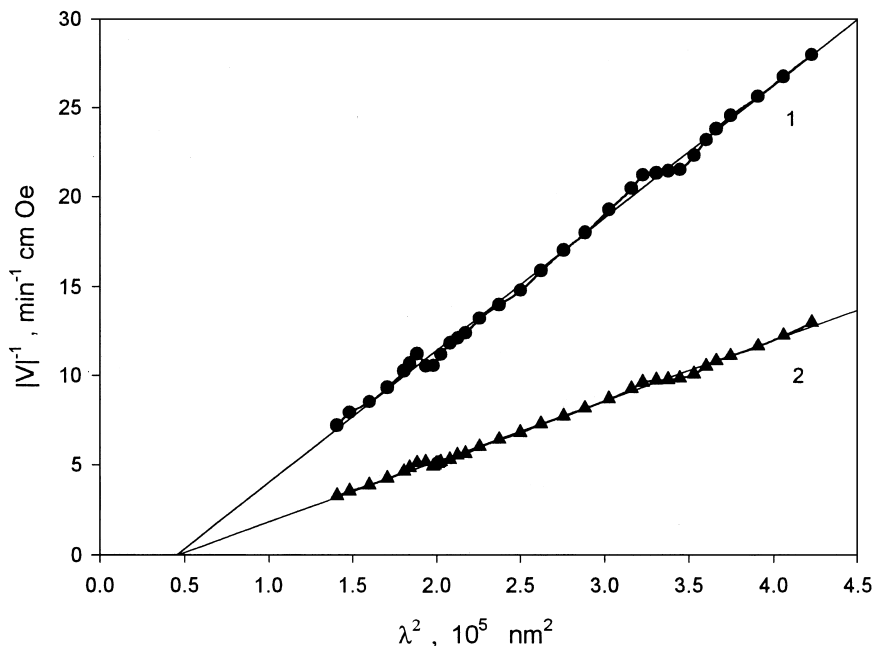


Fig. 3. Dependence of the inverse Verdet constant value on  $\lambda^2$ : (1) 5.13 and (2) 11.46 mol% Pr.

Table 2  
The energies ( $\text{cm}^{-1}$ ) of f-f transitions in  $\text{Pr}^{3+}$  in different matrixes

Transition from $^3\text{H}_4$ to	$\text{Pr}^{3+}$ , free ion [13]	$\text{Pr}^{3+}$ , aqueous solution [15]	$\text{PrCl}_3$ in PVA film [15]	$\alpha\text{-Pr}_2\text{O}_3$ [14]	$\text{Pr}^{3+}$ in silico-phosphate glass [2]	$\text{Pr}^{3+}$ in $\text{LiB}_3\text{O}_5$ glass
$^1\text{G}_4$	9921	–	–	–	–	9881
$^1\text{D}_2$	17334	16800	16830	16977	16920	17006
$^3\text{P}_0$	21390	20750	20630	20618	20880	20746
$^3\text{P}_1$	22007	21300	21370	21097	21430	21008
$^3\text{P}_2$	23160	22520	22420	22271	22500	22522

Eq. (4) from the experiment. It is about  $0.62 \text{ min cm}^{-1} \text{ Oe}^{-1}$  for the sample with 11.46 mol% Pr.

In the absorption spectra (Fig. 1) one can see the narrow lines of the splitting in the region of f-f bands. As it is generally known, a shift of the f-band and maximum in any matrix in comparison with its position for the free RE-ion together with the change of the band intensity reflect the degree of the environment influence on the corresponding f-level.

Table 2 presents the energies of five f-bands in the samples investigated and, for comparison, the energies of these bands in  $\text{Pr}^{3+}$  in different mediums [14,15].

The energies of bands  $^3\text{H}_4 \rightarrow ^3\text{P}_0$  and  $^3\text{H}_4 \rightarrow ^3\text{P}_2$  in the glass investigated coincide accurately with the energies of the same bands in  $\text{Pr}^{3+}$  aqueous solution [16]. The band  $^3\text{H}_4 \rightarrow ^1\text{G}_4$  is influenced by the environment to the least and the band  $^3\text{H}_4 \rightarrow ^3\text{P}_1$ ,  $^1\text{I}_6$  to the utmost extent as it

Table 3

Oscillator strengths of some f–f transitions ( $f \times 10^6$ ) for  $\text{Pr}^{3+}$  ion in the samples investigated and  $\text{Pr}^{3+}$  in aqua solution [16] and in silico-phosphate glass [2]

Transition	$\text{Pr}^{3+}$ in aqua solution	Silico-phosphate glass	Sample with 11.46 mol% Pr
$^1\text{D}_2$	3.12	1.59	2.1
$^3\text{P}_0$	2.52	2.8	1.81
$^3\text{P}_1, ^1\text{I}_6$	6.66	3.68	5.48
$^3\text{P}_2$	14.6	7.45	9.74

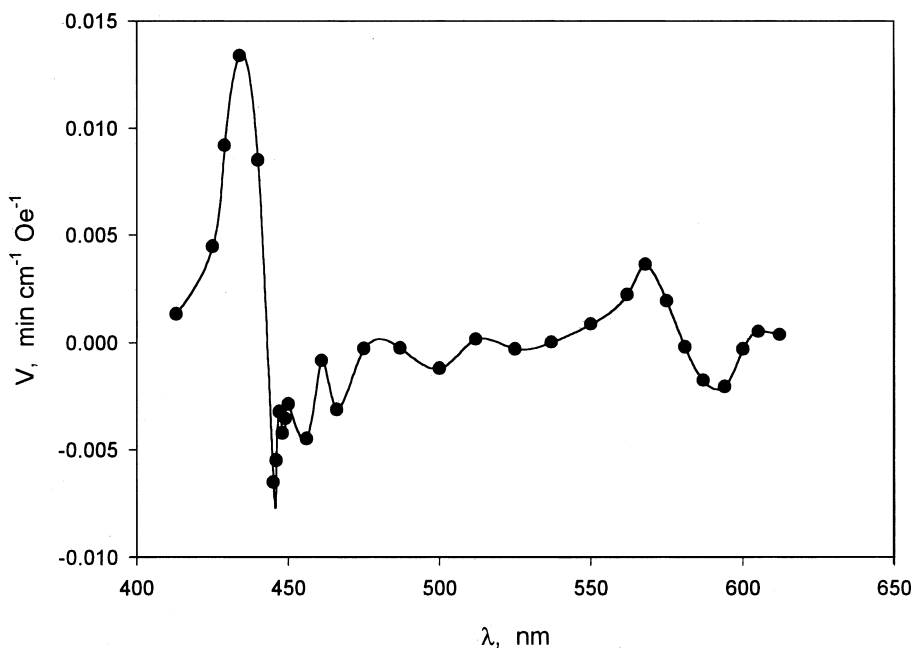


Fig. 4. Spectrum of Verdet constant of f–f transitions in the glass containing 11.46 mol% Pr.

follows from the comparison with the  $\text{Pr}^{3+}$  free ion.

Oscillator strengths calculated according to Ref. [16] are presented in Table 3 for the glasses investigated together with data for Pr aqua solution [14] and Pr containing silicophosphate glass [2]. It is seen that f–f transitions in Pr ions inserted in the glass matrices are weaker in comparison with Pr aqua solution [16]. Among other reasons it can be due to the higher symmetry of Pr ion environment in the glass matrix.

The features in the region of f–f bands are observed in the FR spectrum too. The contribution of

the f–f bands to the FR for the sample with 11.46 mol% Pr is shown in Fig. 4. To receive the contribution of f–f transitions in the FR spectrum the approximation of the FR curves (see Fig. 2) was made and the difference between the calculated values and the experimental data was obtained. The features observed in the FR curves for the f–f transitions correspond to the features in the MCD spectrum, which is shown in Fig. 5. A common view of these spectra agrees well with the data on the MCD in  $\text{Pr}^{3+}$  in different solutions [17]. Note that because of the overlapping of the transitions:  $^3\text{H}_4 \rightarrow ^3\text{P}_0$  (482 nm),  $^3\text{H}_4 \rightarrow ^3\text{P}_1$  (476 nm),  $^3\text{H}_4 \rightarrow$

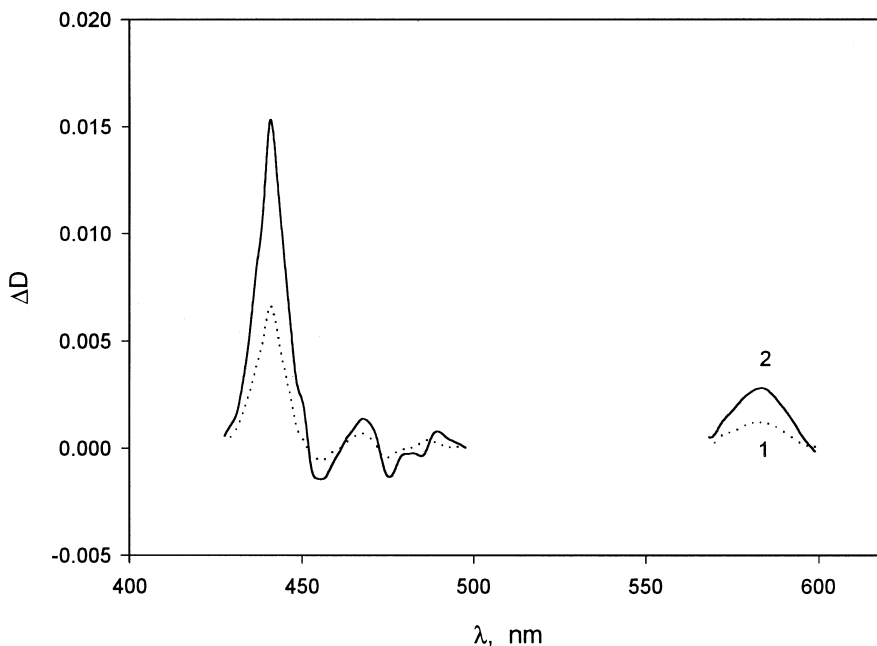


Fig. 5. Spectra of MCD ( $\Delta D = D_- - D_+$ , “+” and “-” refer to the right and left circularly polarized waves): (1) 5.13 and (2) 11.46 mol% Pr.

$^3P_2$  (444 nm) the curves for the FR and MCD are the superposition of the individual curves, which influences the form of the spectrum in this region. So for a further analysis of the FR we consider the short wavelength part of the  $^3H_4 \rightarrow ^3P_2$  transition. In this case  $\lambda_{\text{eff}} = 444$  nm and we may obtain the coefficient  $B$  from (4) the same way as we did it for the f-d transition. The obtained  $B$  value equals  $6.21 \times 10^{-4} \text{ min cm}^{-1} \text{ Oe}^{-1}$ . For the  $^3H_4 \rightarrow ^1D_2$  ( $\lambda_{\text{eff}} = 588$  nm) and  $^3H_4 \rightarrow ^1G_4$  ( $\lambda_{\text{eff}} = 1012$  nm) transitions  $B$  equals  $2.00 \times 10^{-4}$  and  $2.66 \times 10^{-6} \text{ min cm}^{-1} \text{ Oe}^{-1}$ , correspondingly.

Magneto-optical activity, which can be determined as a ratio of the coefficient  $B$  to the intensity (we took the intensity as a band amplitude multiplied by the half of the line width in  $\text{cm}^{-1}$ ) of the corresponding transition, for the f-d transition and for the  $^3H_4 \rightarrow ^3P_2$ ,  $^3H_4 \rightarrow ^1D_2$  and  $^3H_4 \rightarrow ^1G_4$  transitions is equal to  $1.40 \times 10^{-6}$ ,  $2.23 \times 10^{-7}$ ,  $1.72 \times 10^{-7}$  and  $6.14 \times 10^{-9} \text{ min cm Oe}^{-1}$ , correspondingly. Thus, the magneto-optical activity of the f-f transitions is less than the activity of the f-d

transition and its value decreases with the decrease of the transition energy.

### Acknowledgements

This work has been performed with the financial support from the Russian Foundation for Basic Research (Grant No. 99-02-17375).

### References

- [1] C. Gorller-Warland, K. Binnemans, in: K.A. Gschneidner, L. Eyring (Eds.), Handbook on the Physics and Chemistry of Rare Earths, Vol. 25, Elsevier Science, Amsterdam, 1998, pp. 100–264.
- [2] G.T. Petrovskii, I.S. Edelman, T.V. Zarubina, A.V. Malakhovskii, V.N. Zabluda, M.Yu. Ivanov, J. Non-Cryst. Solids 130 (1991) 35.
- [3] V. Zabluda, A. Potseluyko, I. Edelman, A. Malakhovskii, T. Zarubina, G. Petrovskii, M. Ivanov, J. Magn. Magn. Mater. 185 (1998) 207.
- [4] J.I. Qiu, J.B. Qiu, H. Higuchi, Y. Kawamoto, K. Hirao, J. Appl. Phys. 80 (1996) 5297.

- [5] J.I. Qiu, Y. Kawamoto, K. Hirao, *Phys. Chem. Glasses* 38 (1997) 207.
- [6] S.J. Collocott, K.N.R. Taylor, *J. Phys. C* 12 (1979) 1767.
- [7] D.R. MacFarlane, C.R. Bradbury, P.J. Newman, J. Javor-nichky, *J. Non-Cryst. Solids* 213 & 214 (1997) 199.
- [8] K. Binnemans, C. Gorller-Walrand, *J. Alloys Compounds* 250 (1997) 321.
- [9] A.V. Zamkov, V.N. Zabluda, S.A. Parshikov, A.I. Zaitsev. Patent RU 2098366 C1 6 C 03; C3/15.
- [10] M.W. Shafer, J.C.J. Suits, *J. Am. Ceram. Soc.* 49 (1966) 261.
- [11] I.S. Edelman, N.I. Syrova, *Apparatura i metody isledovanija tonkich magnitnykh plenok*, Krasnoyarsk 1967, p. 137.
- [12] S.N. Jaspersen, S.E. Schnatterly, *Rev.Sci.Instr.* 40 (1969) 761.
- [13] G.H. Dieke, in: H.M. Crosswhite, H. Crosswhite (Eds.), *Spectra and Energy Levels of Rare Earth Ions in Crystals*, Wiley, New York, 1968.
- [14] W.B. White, *Appl. Spectrosc.* 21 (1967) 167.
- [15] Y. Kato, K. Nishioka, *Bull. Chem. Soc. Japan* 47 (1974) 1047.
- [16] W.T. Carnall, P.R. Fields, K. Rajnak, *J. Chem. Phys.* 49 (1968) 4412.
- [17] D. Schooley, E. Bunnberg, C. Djerassi, *Proc. Natl. Sci.* 53 (1965) 579.